Applied Energy 171 (2016) 296–313

Contents lists available at ScienceDirect

Applied Energy

journal homepage: www.elsevier.com/locate/apenergy

# Optimization framework for distributed energy systems with integrated electrical grid constraints

Boran Morvaj [a,b,*], Ralph Evins [a,b], Jan Carmeliet [a,c]

[a] Chair of Building Physics, ETH Zürich, Swiss Federal Institute of Technology, Stefano-Franscini-Platz 5, 8093 Zürich, Switzerland
[b] Empa, Urban Energy Systems Laboratory, Überlandstrasse 129, 8600 Dübendorf, Switzerland
[c] Empa, Laboratory of Multiscale Studies in Building Physics, Überlandstrasse 129, 8600 Dübendorf, Switzerland

## HIGHLIGHTS

- Multi-objective optimization framework of distributed energy systems developed.
- Framework combines energy hub, building simulation and distribution grid model.
- Electrical grid constraints integrated by linearizing AC power flow equations.
- Inclusion of grid constraints in the operation schedule reduced emissions 18%.
- Voltage and current variation significantly reduced even with high share of PV.

## ARTICLE INFO

*Article history:*
Received 12 January 2016
Received in revised form 14 March 2016
Accepted 18 March 2016
Available online 23 March 2016

*Keywords:*
Distributed energy systems
AC power flow
Multi-objective optimization
MILP
Genetic algorithm

## ABSTRACT

Distributed energy systems (DES) can help in achieving less carbon-intensive energy systems through efficiency gains over centralized power systems. This paper presents a novel optimization framework that combines the optimal design and operation of distributed energy systems with calculations of electrical grid constraints and building energy use. The framework was used to investigate whether the negative impact of distributed generation on distribution grids can be mitigated and grid upgrades avoided by properly designing and determining operation strategies of DES.

Three new methods for integrating grid constraints were developed based on different combinations of a genetic algorithm and a mixed-integer linear programme. A case study is defined in order to analyze the optimality, accuracy of power flow calculation and solving performance of each method. The comparison showed that each method has advantages and disadvantages and should therefore be chosen based on the application and objectives.

The results showed that the electrical grid constraints have a significant impact on the optimal solutions, especially at high levels of renewable energy use, highlighting their importance in such optimization problems. The inclusion of such constraints directly in the operational scheduling achieved an additional 18% reduction in carbon emissions for a given cost compared to checking the validity of solutions *a posteriori*. Furthermore, by properly designing and determining operation schedules of DES, it is possible to integrated 40% more renewables without grid upgrades.



## 1. Introduction

### 1.1. Background

The European Union has set goals of reducing energy consumption, reducing carbon emissions and improving security of supply. This can be achieved by more efficient use of energy, increased share of renewables and/or use of decentralized energy sources. Distributed energy systems (DES) can help meeting the goals by being more efficient compared to centralized power systems. DES can contain fossil based generators but are often predominantly based on local renewable resources. However, such systems can have negative impact on the existing distribution grids if not designed and managed properly. Manfren et al. [1] analyzed the benefits and drawbacks of distributed energy systems. The main strengths are decreased fossil fuel usage, protection against electric

* Corresponding author at: Urban Energy Systems Laboratory, Swiss Federal Laboratories for Materials Science and Technology, Überlandstrasse 129, 8600 Dübendorf, Switzerland.
*E-mail address:* Boran.Morvaj@empa.ch (B. Morvaj).

http://dx.doi.org/10.1016/j.apenergy.2016.03.090
0306-2619/

system failures through use of local renewable resources and optimal operation of different energy carriers (electricity and heat) to meet the energy demands of the built environment. On the contrary, they can have a negative impact on the grid if integration is not properly managed, such as reverse power flow, voltage rise and cable thermal limits. The evaluation of solutions for decreasing environmental impacts needs to take into account the local and global effects of the proposed solutions. Moreover, optimization approaches are necessary to enable successful application in the field of integration of distributed generation and renewable sources in urban areas. Multiple energy technologies, suitable operating strategies to match time-varying energy demands of buildings to renewable energy sources, and operational limits of the energy carrier infrastructure such as electrical grids should be included for the most efficient integration of DES in the distribution grids and for the decreasing environmental impact.

### 1.2. Previous work

A number of optimization models of distributed energy systems already exist where the objective is to find the optimal design and operation of distributed energy systems according to economic and/or environmental objectives. DER-CAM [2] is an optimization model that determines the optimal capacity and dispatch strategy of distributed generation technologies to minimize global annualized cost on the customer level. Ren and Gao [3] developed a mixed integer linear programming (MILP) model for economic evaluation of DES by selecting appropriate design and operation. Later it was extended to include multi objective optimization considering economic and environmental objectives [4]. Mehleri et al. [5] developed a MILP super-structure model for the optimal design of distributed energy systems, including heating networks. The objective function is the minimization of total annualized cost, and carbon emissions are included as a cost via a carbon tax. Omu et al. [6] developed a model to determine the optimal set of technologies and operation for minimization of annual cost. Holjevac et al. [7] developed a MILP model of a microgrid that determines the optimal microgrid configuration and operation in order to evaluate the flexibility benefits of distributed generation. Chen et al. [8] developed energy management model for determining optimal operating strategies in order to maximize a profit. However, in such publication the constraints of the electrical grid on the integration of local energy sources were not considered, but they assumed the grid to be exogenous and with unlimited capacity. This can lead to solutions that are not possible to integrate in the existing grids and may cause reliability and security issues.

On the other hand, a lot of work has been done in analyzing impact of distributed generation on distribution grid constraints. Calvillo et al. [9] assessed the effects of cable thermal limits on optimal distributed energy resources planning; cable thermal limits are based on maximum energy transfer between households and not on AC power flow calculations. Thomson and Infield [10] looked at the potential technical effects of micro combined heat and power (CHP) on distribution grids for predefined capacities without optimization of operation. Cossent et al. [11] quantified the impact of distributed generation on distribution network costs in three real distribution areas with predefined capacities and no optimization of operation. Liu et al. [12] analyzed impact of CHP, heat pumps and electric boilers on electricity and heat networks. Power flow study was solved using Newton-Raphson iterative method. Mancarella et al. [13] proposed a methodology to model and assess the impact of distributed generation on distribution networks; the capacities of distributed generation are predefined. Baetens et al. [14] developed a tool for simultaneous simulation of thermal and electrical systems at feeder level. Thomson and Infield [15] performed load-flow analyzes for the widespread integration of photovoltaics in distribution systems with predefined capacities and no optimization of operation. Navarro-Espinosa and Mancarella [16] performed high resolution analysis of impact of heat pumps on low voltage networks by solving power flow in OpenDSS. In aforementioned publications there is no optimization included. The capacities are predefined and the power flow study is performed afterwards and cannot influence design or operation. This may provide less efficient solutions and unnecessary grid upgrades.

Integrating AC power flow equations in their original form in the optimization model so that they influence both the design and operation is only possible with a nonconvex mixed integer nonlinear program formulation. However, incorporation of nonconvex constraints leads to a high chance that the global optima are not reached and the solution gives local optima. Moreover, even though there have been recent advances in new solver there is still no efficient solver for such problem which makes the solving computationally demanding and very difficult for larger problems. One of the other approaches used to include power flows in the optimization model is to express them as energy balance for each line or even area as done in [17–21]. In distribution grids with large share of distributed generation, power flows are not necessarily only unidirectional and the inclusion of intermittent sources using energy balance for power flows can lead to incorrect state estimation which can have negative impact on distribution and even transmission grids [22,23].

Another approach is to linearize power flow equations to efficiently integrate them and use them in the optimization problems. The most common linearization of AC power flow equations is DC power flow. However, it assumes that reactive flows are equal to zero and that all voltages are close to nominal value. Also, certain properties of the grid have to be met such as resistance/reactance ratio. As consequence they do not provide any information about voltage magnitudes, reactive power flows and branch, and are not applicable in the distribution grids but are usually applied in transmission lines [24,25]. For distribution grids, linearized AC power flows are required where information about voltages, currents and both active and reactive power flows at each line for each timestep is known [26]. To authors knowledge linearized AC power flows have not yet been combined with the optimal design and operation of DES in any previous work. By obtaining voltages, currents and both active and reactive power flows at each line, it becomes possible to integrate DES in the distribution grids so that the reliability and power quality of the system and the grid is ensured. Also, large voltage fluctuations, exceeding cable thermal limits and transformer limits can be avoided. In that way, additional costs such as upgrade of the grid or replacement of equipment can be avoided.

In conclusion, existing optimization models that find the optimal design and operation of distributed energy systems do not take distribution grid constraints into account and assume that the grid can integrate any amount of local sources. On the other hand, the distribution grid limits are taken into account separately from determining the design and operation of DES, or by combining them in the optimization models in simplified form which does not give all required information. This may lead to inadequate solutions, grid instability, and additional upgrades and maintenance costs.

### 1.3. This paper

In this paper we present a novel optimization framework that incorporates the optimal design and operation of DES with electrical grid constraints (based on AC and linearized AC power flow). The framework advantages over existing literature are shown in Table 1. The framework is applied to a case study to analyze the

**Table 1**
Overview of existing approaches and comparison with the presented framework.

| References | Optimal design and operation | Electric and thermal interaction | Grid constraints | |
|---|---|---|---|---|
| | | | AC power flow | Linearized AC power flow |
| [2–9,17–20] | **Yes** | **Yes** | No | No |
| [10,12–14] | No | **Yes** | **Yes** | No |
| [11,15] | No | No | **Yes** | No |
| [21] | No | **Yes** | No | No |
| Presented framework | **Yes** | **Yes** | **Yes** | **Yes** |

impact of DES on the distribution grid and how can the negative impacts on the grid and grid upgrades be mitigated.

The contributions of this work are: (i) a new framework for coupling grid constraints with the multi objective optimization of design and operation of distributed energy systems in low voltage distribution grids, (ii) a novel way of integrating linearized AC power flows, (iii) a new technique for obtaining branch currents from linearized AC power flow, (iv) inclusion of grid constraints in the operation scheduling, and (v) the application of the framework to a case study to illustrate its importance and investigate the following questions: can the negative impact of distributed generation on distribution grids be mitigated by properly designing DES and determining it operation strategies?; what is the effect of integrating grid constraints in the operation scheduling?; how much more renewable energy can be integrated without the need to upgrade the grid?

In Section 2 outline of the developed optimization framework is given, the components of the framework are defined and three new developed methods for integrating grid constraints are described. A test case is defined in Section 3 in order to compare the methods and analyze the advantages and drawbacks of each method as well as to investigate defined questions. Results on the accuracy of power flow calculations, quality of solution and performance are given followed by a discussion in Section 4. The impact of DES on the distribution grid is analyzed in Section 5. Finally, conclusions regarding the effects of DES on the grid and comparison of methods are given in Section 6.

## 2. Optimization framework

### 2.1. Overview

The optimization framework presented here allows optimizing design and operation of distributed energy systems for various multi-objective economic, environment and technical criteria. An overview is given in Fig. 1. It can be easily adapted and applied to wide range of problems and case studies in urban energy systems. The framework is based on the coupling of an energy hub modelling approach for building systems design, building energy simulations for obtaining heat, cooling and electrical demand profiles, and an electrical grid model for power flow calculation and constraints. An energy hub is a set of multiple conversion and storage technologies which are operated in a controlled manner in order to supply various energy demands [27]. This allows consideration of variable loads and distributed energy resources across multiple buildings. Applications range from a single building to a neighborhood or even city scale. The original formulation of the energy hub has been extended to multiple buildings, and technologies such as gas boiler, combined heat and power (CHP), photovoltaic (PV) and water heat storage have been added. Each building (represented as an energy hub) has to meet its electric and heat demands based on the available inputs using conversion technologies while minimizing defined objective(s). This can be easily further extended to include any technology or storage as well as any type of energy demand. An example of design and operational variables that can be used is shown in Table 2.

Hourly demand profiles are obtained from the results of building energy simulations where each building is modelled individually. Input data for building simulations includes characteristics of construction materials, geometry, lighting and equipment, number of occupants and their schedules, and weather data. Buildings are connected to distribution grid and can export or import electricity from the grid. Buildings can act as individuals where cost and carbon emissions of electricity import/export are summed for each building individually, or they can form a microgrid with common objective(s) where the cost and carbon emissions of electricity import/export are summed over the whole grid and only flows leaving the microgrid boundary are accounted for. The model of the distribution grid is built based on the network topology, line and transformer parameters. For each building and timestep, net electricity balance (electric demand minus local generation) is calculated in order to compute if the building is an injection node or a load node from the distribution grid point of view. This is followed by a sequential power flow study for each timestep to obtain steady-state variables such as voltage magnitude and angles, active and reactive branch power and branch current magnitude. Variables are evaluated with respect to operational stable limits which represent global constraints for the optimization process, and thus influence the optimal solutions. Optimization can be for one or more objectives such as cost minimization, optimal power flow, emissions minimization, and microgrid autonomy. Additionally, the optimization can be performed for any timescale (from seconds to hours). However, smaller timesteps increases the complexity of the model and it can become computationally intractable.

### 2.2. Energy hub model

The energy hub is a modelling formulation which assigns the conversion and storage of multiple energy streams in order to meet various demands. The original formulation was further developed and applied to buildings and extended to determine the optimal design of energy technologies and storage devices as well as the optimal dispatch of different energy streams. The problem is formulated as a mixed-integer linear programme (MILP). The main advantage is that the detailed modelling of each technology is not needed but is represented as conversion efficiency between multiple input energy sources to multiple outputs. However, solving the model requires linearity so efficiencies are assumed to be constant. If more detailed modelling is needed, advanced linear programming methods such as piece-wise linearization can be used. It is assumed that a suitable control approach can be used for the real system that can match the optimized operation schedule, which is reasonable at hourly resolution. The energy hub formulation can be used for individual buildings or sets of buildings up to neighborhood scale.

In this optimization framework, the energy hub model is used for a number of buildings that can interact. For each building $i$ the optimal design and operation of the technologies is determined in order to satisfy the demand profiles obtained from a building energy simulation.

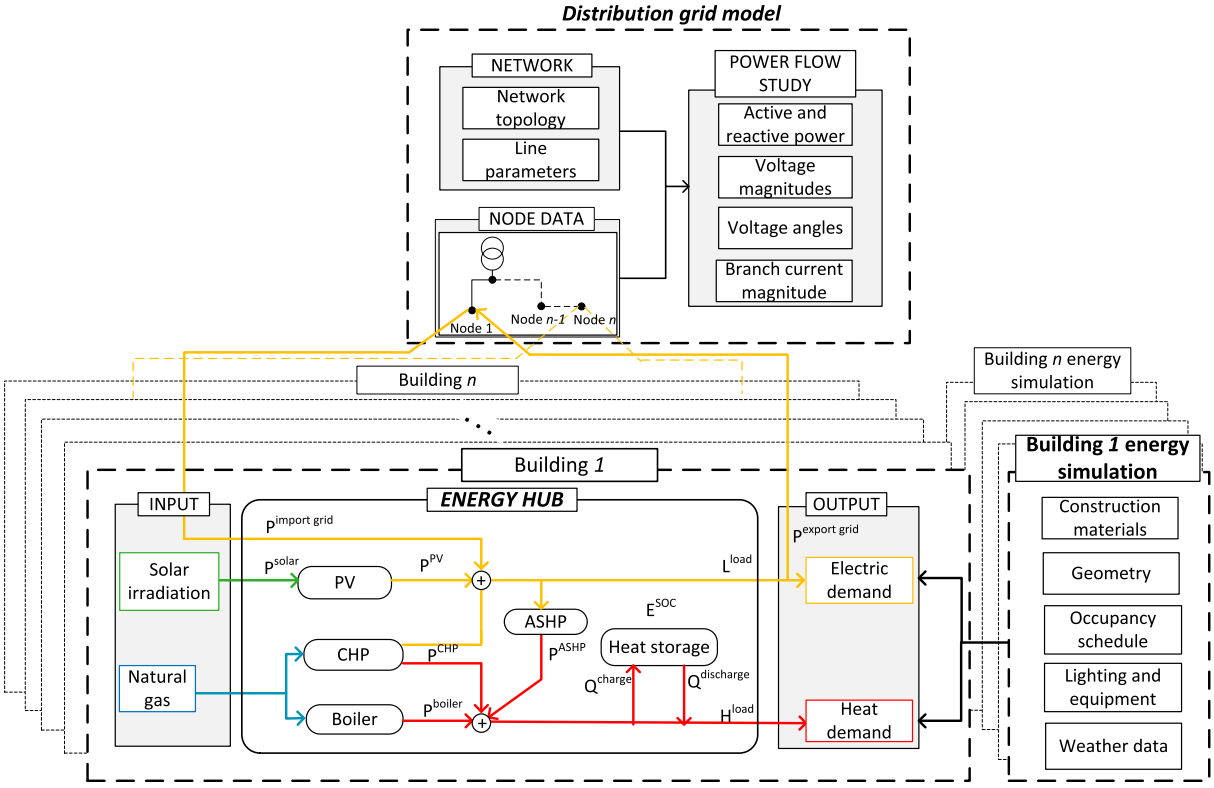


**Fig. 1.** Overview of the framework for the optimization of distributed energy systems under electrical grid constraints.

**Table 2**
Example of design and operational variables.

| Design variables | ∀ building | ∀ timestep |
|---|---|---|
| Capacity of combined heat and power plant | x | - |
| Capacity of photovoltaics | x | - |
| Capacity of gas boiler | x | - |
| Capacity of heat storage | x | - |
| *Operational variables* | | |
| Electricity output of combined heat and power | x | x |
| Heat output of combined heat and power | x | x |
| Electricity output of photovoltaics | x | x |
| Heat output of gas boiler | x | x |
| State of charge of heat storage | x | x |
| Charge of heat storage | x | x |
| Discharge of heat storage | x | x |
| Electricity sold to electrical grid | x | x |
| Electricity purchased from electrical grid | x | x |

Each technology has a fixed efficiency between $k$ inputs $P_k^{\text{input}}$ (e.g. natural gas, irradiation for PV) and outputs electricity demand $L^{\text{load}}$ and heat demand $H^{\text{load}}$. Each conversion technology *tech* is represented by a dispatch variable $P^{\text{tech}}$, and energy storages *stor* are charged and discharged by variables $Q_{\text{stor}}^{ch}$ and $Q_{\text{stor}}^{\text{dis}}$. All variables are determined for each building $i$ and for a number of timesteps $t$.

The electricity demand has to be met using electricity imported from the grid $P^{\text{import grid}}$ (minus electricity exported to the grid $P^{\text{export grid}}$) or by technologies and storages with electricity output:

$$L(i,t) = P^{\text{grid import}}(i,t) + \Theta_{\text{tech}} \times P^{\text{tech}}(i,t) - P^{\text{grid export}}(i,t) + n_{\text{stor}}^{\text{dis}} Q_{\text{stor}}^{\text{dis}}(i,t) - n_{\text{stor}}^{\text{ch}} Q_{\text{stor}}^{\text{ch}}(i,t) \quad (1)$$

where $\Theta_{\text{tech}}$ is a matrix of conversion efficiencies for each technology and $n_{\text{stor}}^{\text{dis}}$, $n_{\text{stor}}^{\text{ch}}$ are discharging and charging efficiencies of energy storages. It is not allowed to export and import electricity from the grid, or to charge and discharge storages at the same time.

Similarly, the heat demand has to be met by technologies and storages with heat energy output:

$$H(i,t) = \Theta_{\text{tech}} \times P^{\text{tech}}(i,t) + n_{\text{stor}}^{\text{dis}} Q_{\text{stor}}^{\text{dis}}(i,t) - n_{\text{stor}}^{\text{ch}} Q_{\text{stor}}^{\text{ch}}(i,t) \quad (2)$$

The same operational constraints apply as for the electricity balance (Eq. (1)).

Each storage is characterized by the state of charge variable $E_{\text{stor}}^{\text{SOC}}$, and continuity is expressed by the amount of energy at the next timestep that is equal to the amount at the current timestep plus the charged amount minus discharged amount:

$$E_{\text{stor}}^{\text{SOC}}(i,t+1) = E_{\text{stor}}^{\text{SOC}}(i,t) + n_{\text{stor}}^{\text{dis}} Q_{\text{stor}}^{\text{dis}}(i,t) - n_{\text{stor}}^{\text{ch}} Q_{\text{stor}}^{\text{ch}}(i,t) \quad (3)$$

The objective function to be minimized is the sum of the input energy streams multiplied by coefficients $C_k$:

$$\min f = \sum C_k \times P_k^{\text{input}} \quad (4)$$

Depending on what $C_k$ represents, different objective functions can be defined. If $C_k$ represents prices, the objective function gives the minimization of operating costs. If $C_k$ represents carbon factors, the objective function gives the minimization of annual carbon emissions. The problem can also be formulated as multi-objective to minimize two objective functions simultaneously.

In this paper, a multi-objective optimization of the total cost (investment and operational) and carbon emissions is performed. For multi-objective optimization using MILP, the $\varepsilon$-constraint method [28] is used, which minimizes the primary objective function while the secondary objective function is translated into additional inequality constraints for which the limit ($\varepsilon$) is varied to obtain a trade-off front of solutions:

$$\text{minimize } \{F_1(x)\} \text{subject to } F_2(x) \leqslant \varepsilon_a \qquad \forall a \in [1,\ldots,n] \quad (5)$$

The number of values of $\varepsilon$ corresponds to the number of points on the front; they are usually selected to be evenly spaced between the minimum and maximum values of the objective $F_2$.

Additional design and operational constraints can be added to the model as required: e.g. minimum load constraints; if the technology or storage is present it had to be between lower and upper bound; the output has to smaller or equal to the installed capacity; maximal charging and discharging rate etc. For more details about energy hub formulation and description of detailed model which includes advanced design and operational constraints, the reader is referred to [29,30].

### 2.3. Integrating distribution grid constraints

We present three new methods for grid constraints to be integrated in the optimization model (shown in Fig. 2). All methods have advantages and disadvantages and influence the optimization process in a different way. The first method (a) is based on a bi-level optimization approach using heuristic for design and deterministic optimization algorithm (MILP) for operation (described in the next section) where the grid model and constraints are separate from the energy hub model. Each proposed optimal design and operation schedule is checked against power flow and stability constraints and penalized accordingly. The power flow equations are solved using the full non-linear formulation which ensures high accuracy. The drawback is that the constraints cannot directly influence the optimal design and operation, and represent an *a posteriori* check. The second method (b) is based on the integration of the alternative current (AC) power flow equations and constraints within the energy hub model by linearizing the equations. This way the constraints directly influence the optimal design and operation of the DES and global optima are guaranteed. The drawback is that through linearization of the power flow equations some accuracy is lost. The third method (c) combines aspects of the first two methods by using heuristic for the design, MILP with linearized AC power flow and non-linear formulation of AC power flow for checking the accuracy of the solution from the grid perspective.

#### 2.3.1. Bi-level method

The bi-level optimization method consists of two optimization levels within one optimization process (see Fig. 3). The main level conducts the design optimization, while the sublevel conducts the operational optimization. In the main level, a multi-objective genetic algorithm NSGA-II [31] is used for decision variables concerning design of the considered technologies for each building. Genetic algorithms are a metaheuristic belonging to the class of evolutionary methods based on iteratively improving solutions by use of recombination and mutation. A population of solutions is ranked by fitness and the best are used to form a new population. NSGA-II is commonly used for multi-objective design optimization. The population is initialized using a Sobol sequence, a type of quasi-random low-discrepancy sequence that fills an $n$-dimensional space in a uniformly distributed manner. This ensures that the initial design space is evenly covered by starting points and there are no potential 'lumps' of the initial solutions happening. The design variables are passed to the sublevel to perform the fitness evaluation of each individual. The sublevel is a MILP energy hub model where the optimal operation is determined and assigned design variables from the main level represent operational constraints. The objective of the optimization is minimization of the operational cost. Additionally, the difference between electricity demand and electricity generated locally from distributed energy resources is calculated for each building for each timestep. If the result is positive, it means the building is importing the electricity from the grid and represents nodal load from the grid point of view; if it is negative it means it is exporting electricity and represents a nodal injection. After the sublevel optimization, the total cost (operating plus investment costs), total carbon emissions and node injections/loads are sent back to the main level. Next, node injection/load values are passed to a distribution grid model built in MATPOWER in Matlab [32]. Steady state nonlinear AC power flow calculations are solved for each timestep using the Newton-Raphson method. The nonlinear equations for the AC power flow on arc $(n, m)$ are expressed as:

$$P((n,m)) = U_n^2 \cdot G_{nm} - U_n \cdot U_m \cdot G_{nm} \cdot \cos(\vartheta_n - \vartheta_m) - U_n \cdot U_m \cdot B_{nm} \cdot \sin(\vartheta_n - \vartheta_m) \quad (6)$$

$$Q((n,m)) = -U_n^2 \cdot B_{nm} + U_n \cdot U_m \cdot B_{nm} \cdot \cos(\vartheta_n - \vartheta_m) - U_n \cdot U_m \cdot G_{nm} \cdot \sin(\vartheta_n - \vartheta_m) \quad (7)$$

where $P$ is active power, $Q$ is reactive power, $U$ is voltage magnitude, $G$ is line conductance, $B$ is line susceptance and $\vartheta$ is voltage angle. The solutions are checked to see if they violate grid constraints such as voltage difference bigger than ±10% of the nominal voltage and branch currents higher than the cable thermal limit or circuit breaker limit. If they violate, a penalty value of difference between calculated and the target value is assigned to the solution. The next step is ranking and selection calculated using the standard NSGA-II approach. Individuals without grid constraint violations always dominate individuals with violations, and individuals with smaller violations dominate individuals with bigger violations. An individual is said to dominate another if the objective functions value is no worse than the other and at least in one of its objective functions value is better than the other. This way non-violating solutions are always preferentially selected and eventually violating solutions will not be included in the current population. Crossover and mutation is performed on the individuals selected to form the new population. The optimization is stopped and final Pareto front solutions are obtained after a given number of generations.

The bi-level method is governed by the NSGA-II algorithm which is a type of heuristic optimization algorithm. It provides good solutions with relatively quick convergence. The advantage is that it uses accurate AC power flow calculations and can efficiently solve both small and large problems. However, finding the global optimum cannot be guaranteed. Also, the optimal operation cannot be influenced by grid constraints, which may hinder the search for the best solutions.

#### 2.3.2. MILP with integrated linearized AC power flows method

The most common linearized formulation of the power flow equations is DC power flow. It is based on the following assumptions:

- Resistance is significantly less than reactance and therefore conductance $G$ is assumed to be zero.
- Voltage angle differences are very small therefore $\sin(\vartheta_n - \vartheta_m) \approx \vartheta_n - \vartheta_m$ and $\cos(\vartheta_n - \vartheta_m) \approx 1$.
- In the per-unit system voltage magnitudes $U_n$ and $U_m$ are very close to 1.0.

The power flow equations (Eqs. (6) and (7)) can therefore be transformed into DC power flow equations expressed as:

$$P((n,m)) = B_{nm} \cdot (\vartheta_n - \vartheta_m) \quad (8)$$

$$Q((n,m)) = 0 \quad (9)$$

This formulation is most commonly used for real-time dispatch, contingency analysis and techno-economic analysis of the power system at high voltage where they are reasonably accurate. They are fast to calculate and non-iterative. However, DC power flow looks only at active power flows, neglecting voltage support, reactive power management and transmission losses. Furthermore,

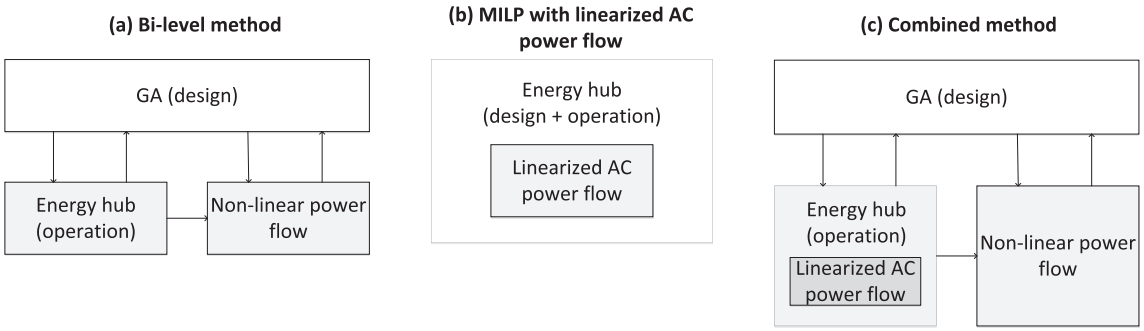


**Fig. 2.** Three new methods for integrating distribution grid constraints.

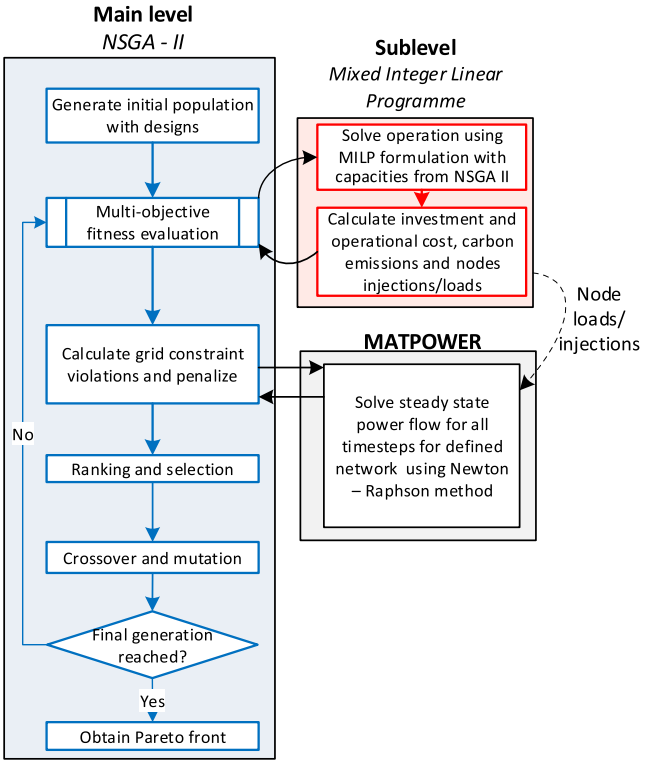


**Fig. 3.** Overview of the optimization process for bi-level method.

reactive flows Q are omitted and that the modelled network has to fulfil specific properties (e.g. resistance/reactance ratio). Therefore, DC power flow is not suitable for distribution grids that do not fulfil the requirements. For more details about drawbacks of DC power flow reader is referred to [25].

In this paper we use an approximation of the AC power flow as presented in [26] in order to obtain both active and reactive power flows. Similar assumptions are made as for DC linearization but without setting $\Delta U_{ij}$ and conductance $G_{ij}$ to zero. The linearized AC power flow equations on arc $(n, m)$ can be then expressed as:

$$P((n,m),t) = U_0 \cdot G_{nm} \cdot \Delta U_{nm,t} - U_0^2 \cdot B_{nm} \cdot \Delta\vartheta_{nm,t} \quad \forall t \tag{10}$$

$$Q((n,m),t) = -U_0 \cdot B_{nm} \cdot \Delta U_{nm,t} - U_0^2 \cdot G_{nm} \cdot \Delta\vartheta_{nm,t} \quad \forall t \tag{11}$$

$$\sum P(n,t) = \sum_i P_{i,t,\text{load}} - \sum_i P_{i,t,\text{gen}} \quad \forall n,t \tag{12}$$

$$\sum Q(n,t) = \sum_i Q_{i,t,\text{load}} - \sum_i Q_{i,t,\text{gen}} \quad \forall n,t \tag{13}$$

Symmetric power flow is assumed as in DC power flow but reactive power flow can now be calculated. The linearized AC power flow equations are integrated in the energy hub model where Eqs. (12) and (13) are expressed as:

$$\sum P(n,t) = L_{i,t}^{\text{load}} - \sum_{\text{ota}} P_{\text{gen}}^{\text{tech}}(i,t) + \sum_{\text{ota}} P_{\text{con}}^{\text{tech}}(i,t)$$

$$\forall n,i,t \text{ and ota} \in \text{technologies that produce/consume active power} \tag{14}$$

$$\sum Q(n,t) = QL_{i,t}^{\text{load}} - \sum_{\text{otr}} P_{\text{gen}}^{\text{tech}}(i,t) + \sum_{\text{otr}} P_{\text{con}}^{\text{tech}}(i,t)$$

$$\forall n,i,t \text{ and otr} \in \text{technologies that produce/consume reactive power} \tag{15}$$

where *gen* denotes generation and *con* consumption. From the Eqs. (10), (11), (14) and (15) voltage magnitudes ($U$), voltage angles ($\vartheta$), branch active power $P((n,m),t)$ and branch reactive power $Q((n,m),t)$ are obtained during the optimization but no branch current. In the low voltage distribution grid, information about branch power flow and voltage magnitude is not sufficient for achieving stable operation; branch current is also needed to ensure operating conditions remain within cable thermal limits and circuit breaker nominal currents. The current in branch $(n, m)$ at timestep is equal to:

$$I_{nm,t} = \frac{\Delta U_{nm}}{Z_{nm}} = \frac{U_n \cdot \cos\vartheta_n + i \cdot U_n \cdot \sin\vartheta_n - U_m \cdot \cos\vartheta_m - i \cdot U_m \cdot \sin\vartheta_m}{R_{nm} + i \cdot X_{nm}} \quad \forall\, n,t \tag{16}$$

where $R$ is the line resistance and $X$ is the line reactance. This expression is nonlinear, and has to be linearized in order to obtain branch current as part of a linear optimization. For this, a series of approximations and linearization techniques are applied as follows:

1. Voltage magnitude difference is small therefore $\sin(\vartheta_n - \vartheta_m) \approx \vartheta_n - \vartheta_m$ and $\cos(\vartheta_n - \vartheta_m) \approx 1$.
   This gives:

$$I_{nm,t} = \frac{\Delta U_{nm}}{Z_{nm}} = \frac{U_n + i \cdot U_n \cdot \vartheta_n - U_m - i \cdot U_m \cdot \vartheta_m}{R_{nm} + i \cdot X_{nm}} \tag{17}$$

Complex numbers are not supported by linear programming, therefore the current has to be expressed explicitly as real and imaginary part and the parts are treated separately:

$$\begin{aligned} I_{nm,t} &= \frac{U_n + i \cdot U_n \cdot \vartheta_n - U_m - i \cdot U_m \cdot \vartheta_m}{R_{nm} + i \cdot X_{nm}} \cdot \frac{R_{nm} - i \cdot X_{nm}}{R_{nm} - i \cdot X_{nm}} \\ &= \frac{R_{nm} \cdot (U_n - U_m) + X_{nm} \cdot (U_n \cdot \vartheta_n - U_m \cdot \vartheta_m)}{R_{nm}^2 + X_{nm}^2} + i \\ &\quad \cdot \frac{-X_{nm} \cdot (U_n - U_m) + R_{nm} \cdot (U_n \cdot \vartheta_n - U_m \cdot \vartheta_m)}{R_{nm}^2 + X_{nm}^2} \\ &= Re(I_{nm,t}) + Im(I_{nm,t}) \end{aligned} \tag{18}$$

2. The expression is still nonlinear due to the product of two continuous variables $U \cdot \vartheta$. A linear programming technique for the transformation of a product of two continuous variables into a separable form [33] is used. Two new continuous variables $a$ and $b$ are introduced and defined as:

$$a = \frac{1}{2} \cdot (U + \vartheta) \tag{19}$$

$$b = \frac{1}{2} \cdot (U - \vartheta) \tag{20}$$

$$U \cdot \vartheta = a^2 - b^2 \tag{21}$$

3. The terms $a^2$ and $b^2$ have to be linearized. We know that $U$ is close to 1 p.u. and $\vartheta$ is close to 0, therefore $a \approx 0.5$ and $b \approx 0.5$. We use first order Taylor series around the point 0.5 for variables $a^2$ and $b^2$, and get the following terms:

$$f(0.5) + \frac{f'(0.5)}{1!} \cdot (a - 0.5) = -0.25 + a \tag{22}$$

$$f(0.5) + \frac{f'(0.5)}{1!} \cdot (b - 0.5) = -0.25 + b \tag{23}$$

Therefore, we can express product of voltage magnitude and voltage angle as:

$$U \cdot \vartheta = a^2 - b^2 = -0.25 + a + 0.25 - b = a - b = \vartheta \tag{24}$$

The current equation can now be expressed in a linearized form:

$$I_{nm,t} = \frac{R_{nm} \cdot (U_n - U_m) + X_{nm} \cdot (\vartheta_n - \vartheta_m)}{R_{nm}^2 + X_{nm}^2} + i \cdot \frac{-X_{nm} \cdot (U_n - U_m) + R_{nm} \cdot (\vartheta_n - \vartheta_m)}{R_{nm}^2 + X_{nm}^2} \tag{25}$$

4. Current is a complex number consisting of the magnitude and phase angle. However, only current magnitude is needed. Therefore, the absolute value of the complex number is needed, which includes quadratic terms of the real and imaginary parts. Also, this way the imaginary unit in the imaginary part is eliminated and can be handled by linear programming. Since the current will vary from zero to some nominal value, the only solution for approximating the quadratic function is to use a piecewise linear formulation. The current can be positive or negative depending on the direction and in order to reduce the size of the model, first an absolute value of both real and imaginary parts of the current is taken. The absolute value function is nonlinear, and a linear programming approximation is performed by introducing new variables $\varphi$ and $\omega$ and including them in the objective function:

$$\varphi \geqslant Re(I_{nm,t}), \quad \omega \geqslant Im(I_{nm,t}) \tag{26}$$

$$\varphi \geqslant -Re(I_{nm,t}), \quad \omega \geqslant -Im(I_{nm,t}) \tag{27}$$

where $\varphi$ is absolute value of real part of the branch current and $\omega$ is absolute value of imaginary part of the branch current.

5. The next step is to approximate the squared absolute real and imaginary part of the current by piecewise linear formulation. This is done by dividing the quadratic function into $n$ pieces that are approximated by straight lines. The number of pieces depends on the accuracy needed. The $\lambda$-formulation method was used for piecewise approximation written as following:

$$\lambda_1 f(x_1) + \lambda_2 f(x_2) + \ldots \lambda_n f(x_n) = \varphi^2 \text{ or } \omega^2 \tag{28}$$

$$\lambda_1 x_1 + \lambda_2 x_2 + \ldots \lambda_n x_n = \varphi \text{ or } \omega \tag{29}$$

$$\lambda_1 + \lambda_2 + \ldots \lambda_n = 1 \tag{30}$$

where $x_n$ is $n$th breakpoint, $f(x_n)$ is the corresponding squared value and $\lambda_n$ are nonnegative weights such that their sum is 1 with at most two adjacent $\lambda$s greater than zero.

6. Squared real and imaginary part has to be summed in order to obtain squared value of the current which can be then limited by the nominal current expressed as squared value:

$$I_{nm,t}^2 = \varphi^2 + \omega^2 \leqslant I_{\text{nominal}}^2 \tag{31}$$

The approximations are performed for each branch and for each timestep. The terms $\omega$ and $\varphi$ are added to objective function and multiplied by a very small value. This way there is no impact on the objective value and no additional binaries are needed and which would increase computational time. The terms $\varphi^2$ and $\omega^2$ are convex and the objective is to minimize a separable functions, therefore it is not required that at most two adjacent $\lambda$'s are greater than zero.

MILP is a deterministic optimization technique, which means that the global optimum is guaranteed. Furthermore, the optimal operation can be directly influenced by the distribution grid constraints thus providing better solutions compared to *a posteriori* check in the bi-level method. For example, in the bi-level method the proposed design and operation is checked if it violates grid constraints. A solution will be discarded even with a small violation. However, in this method because grid constraints are integrated in the operation optimization, a small shift in scheduling without impact on the design can make the solution possible from the grid perspective. On the other hand, the accuracy of the linearization and approximation methods applied may introduce an error (analyzed in the result section). Also, for large problems it can become computationally intractable due to the large amount of RAM required.

#### 2.3.3. Combined method

This method combines the bi-level and MILP with integrated linearized AC power flow methods. It consists of two optimization levels, as with the bi-level method. NSGA-II assigns the design variables which are passed to the sublevel MILP energy hub model, where the optimal operation is found based on proposed design that represents operational constraints. The distribution grid constraints are imposed by integrating linearized AC power flow approximations as described in the previous section. The objective values and proposed operation from the MILP model are passed back to the main level (NSGA-II) where the operation is checked against the grid constraints by solving the nonlinear AC power flow equations. This way the operation is directly influenced by the grid constraint (in linearized form), which provides better solutions. Also, it ensures that the solutions are feasible with certainty from the grid perspective. Furthermore, it can efficiently solve both small and large problems but takes longer time compared to the bi-level method due to the algorithm and the model being more complex. On the other hand, finding the global optimum is still not guaranteed.

## 3. Test case

For the test case a multi-objective optimization of cost and carbon emissions was performed on an hourly timescale. The test case consists of five residential buildings – two single family houses and three apartment buildings. The construction and geometry parameters of the buildings are given in Table 3. The buildings were modelled in EnergyPlus [34]. Varying schedules were defined for heating set points, domestic hot water (DHW), lighting and occupancy. Weather data for Zürich, Switzerland was used for simulation. The simulation was run with an hourly timestep for the whole year. In order to decrease the computational time and complexity of the problem, electricity and heat demand for each month were represented by an average 24 hourly profiles and taken as inputs for the optimization model (in total 288 timesteps).

**Table 3**
Construction parameters of residential buildings.

| Parameter | Value |
|---|---|
| Window area | 27 $m^2$/floor |
| Wall construction | 1.7 W/$m^2$ K |
| Roof construction | 2.75 W/$m^2$ K |
| Floor construction | 2.85 W/$m^2$ K |
| Window glass | 5 W/$m^2$ K |
| Heat consumption | 121 kW h/$m^2$/y |
| Total consumption | 168 kW h/$m^2$/y |

Electricity and heat demand (consisting of heating and DHW demands) are shown in Figs. 4 and 5. Letters in brackets correspond to the letter for each building in Fig. 6.

Assumed efficiencies, capacity bounds and costs for each technology are shown in Table 4. The carbon factor used for natural gas is 0.202 kg $CO_2$/kW h [35] and for electricity 0.5 kg $CO_2$/kW h [36]. Only operating emissions are taken into account and not life cycle emissions. The electricity grid price is 0.2 €/kW h [37] and natural gas price is 0.08 €/kW h [37]. The price for selling electricity back to the grid was assumed not to be subsidized and is taken to be 0.08 €/kW h. It was assumed that there is carbon 'credit' equal to the electricity carbon factor given for exported electricity (only for electricity generated from PV), which decreases the total carbon emissions of the microgrid. The prices are taken to be constant throughout the optimization period and for potential variations uncertainty optimization has to be applied. However, this framework is based on the deterministic optimization and price variation is not considered. Furthermore, if CHP load is higher than the minimum, its efficiency is constant i.e. independent of the load. Also, it is assumed that solar irradiation, electricity and heat demand are known with certainty. This allows the linearity of the model to be maintained, an assumption which is used in almost all energy hub studies in the literature.

Low voltage distribution grid parameters and topology is based on the low voltage microgrid network benchmark [38], which is shown in Fig. 6 along with building peak electricity demands and floor area. Only the residential feeder was considered supplying the five residential buildings. Building demands as well as floor area were scaled to meet the peak electricity demands of each building as specified in the microgrid network benchmark. It is assumed that the network is balanced, therefore only a single phase is taken into account. The nominal voltage of the grid is assumed to be 0.4 kV. Table 5 shows the line parameters resistance and reactance. The power factor was assumed to be 0.85 lagging and for distributed generation unity. Optimal solutions are not allowed to violate following constraints: voltage more than ±10% of the nominal voltage and line current higher than 250 A.

The parameter values of NSGA-II algorithm used can be seen in Table 6.

## 4. Comparison of methods

Results are presented for each method in turn. An error analysis for the linearized calculation of AC power flow is also presented. Furthermore, results of the three methods are compared and analyzed. The final section shows example solutions obtained with each method.

### 4.1. Bi-level method

Fig. 7 shows the Pareto front of solutions obtained (green[1] dots) plotted against the two objectives of annualized total cost and annualized carbon emissions. There were 93 unique solutions. Gray dots show all evaluated solutions. In total there were 10,000 fitness function evaluations. Red crosses indicate solutions that violated current magnitude constraint and blue circles indicate solutions that violated voltage magnitude constraint. The proposed design and optimal operation is not possible in the existing distribution grid for the violating solutions.

The Pareto front ranges from the lowest cost design of 72 k€/a with carbon emissions of 220 tons/a. The carbon emissions can be decreased by 50% to 110 tons/a (lowest carbon solution) but the total cost increases by 28% to 90 k€/a. The negative values come from the assumption that carbon is accounted for electricity exported to the grid. This is in line with the emissions metrics for net zero energy buildings or positive energy buildings where the carbon emissions performance of the building is determined by difference between emissions of used energy and exported energy [39]. Looking at solutions that violated grid constraints, they are mostly clustered at the lower right part of the objective space outside the Pareto front area. They are solutions with lower carbon emissions achieved by integrating more distributed generation into the grid. Most of the grid violations are high branch currents. The voltage magnitude violations occur at the lowest carbon emissions where high amount of distributed generation is integrated.

### 4.2. MILP with linearized AC power flow

Fig. 8 shows the Pareto front of solutions (blue dots) for this method. The lowest cost solution is 70 k€/a with carbon emissions of 233 tons/a. The carbon emissions can be decreased by 61% to 90 tons/a but the total cost increases by 27% to 89 k€. The optimal solutions were obtained by finding the minimum and maximum carbon emissions objective and dividing the range by 28 points which represent $\varepsilon$-constraint for carbon emissions objective while minimizing total cost.

### 4.3. Error in linearization of AC power flows

The accuracy of the integrated linearized AC power flow in the MILP model has been evaluated for a single MILP optimization run, by comparing it to the results of a non-linear AC power flow as benchmark. The non-linear AC power flow equations were solved with the Newton-Raphson method using Matpower in MATLAB, same as for the bi-level method. The current and voltage magnitude results are given in Figs. 9 and 10. The linearized current magnitude matches very well the current magnitude from the non-linear AC power flow calculation (see Fig. 9). There are some discrepancies for lower values in branches 3–4, 5–6 and 6–7, however these are not important since only the maximum current magnitude is of interest because it is one of the key parameters of the electrical grid and equipment. The error comes from using fewer pieces for lower values in the piece wise linearization of the quadratic function (Eqs. (28)–(30)). Absolute error is shown, since relative error is not relevant, only the absolute current magnitude. The absolute error of the critical high magnitude values is small (on average less than 200 $A^2$), which means that the series of approximations used for the current magnitude do not introduce significant error. Voltage magnitudes fit almost perfectly as seen in Fig. 10. The relative error is always below 0.1%.

However, in this test case voltage magnitudes are always close to the nominal value of 1 p.u., where the linearization is most accurate. In order to evaluate the accuracy for all stable operation points, a large number of simulation runs were performed and compared to non-linear AC power flow as a benchmark. Voltage and current magnitude correlations and non-linear values against linear values are plotted in Fig. 11. Bus voltages are evaluated for

[1] For interpretation of color in Figs. 7, 8 and 12, the reader is referred to the web version of this article.

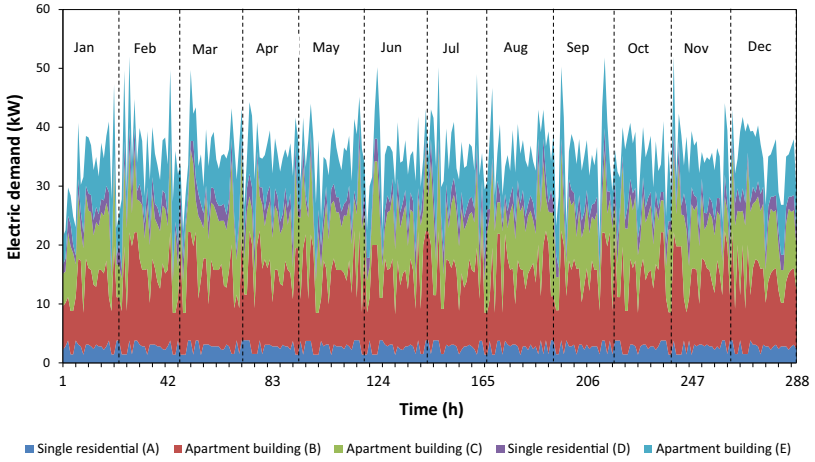


**Fig. 4.** Simulated electricity demand for 5 residential buildings.

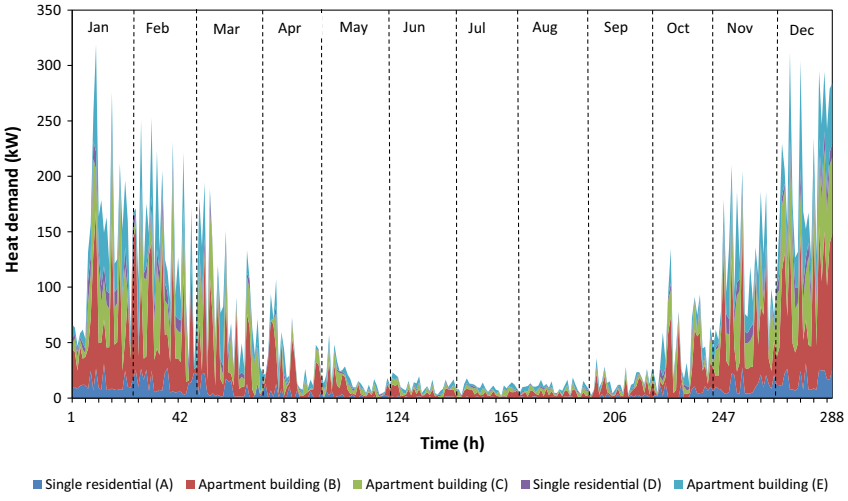


**Fig. 5.** Simulated heat demand for 5 residential buildings.

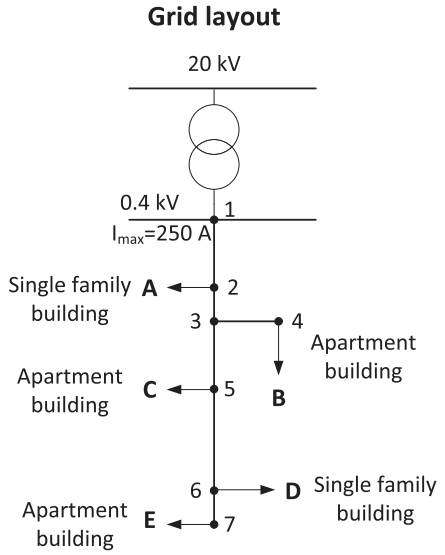


| Building | Peak electricity | Floor area |
|---|---|---|
| A | 5 kVA | 150 $m^2$ |
| B | 24 kVA | 700 $m^2$ |
| C | 18 kVA | 600 $m^2$ |
| D | 5 kVA | 150 $m^2$ |
| E | 16 kVA | 550 $m^2$ |

**Fig. 6.** The configuration of the low voltage distribution grid from [26] and associated building data.

**Table 4**
Efficiencies, capacity bounds and costs for each technology, with sources.

| Technology | Efficiency | Capacity bounds | Fixed cost | Linear cost |
|---|---|---|---|---|
| CHP [3] | $\eta_{el}$: 30%. HER: 2 | 0–100 kW | 1000 € | 500 €/kW |
| Gas boiler [6] | 80% | 0–200 kW | 50 € | 50 €/kW |
| PV [43] | 15% | 0–225 kWp | 1500 € | 600 €/m$^2$ |
| Thermal storage [44] | 99% per timestep | 0–60 kW h | 100 € | 70 €/kW h |

**Table 5**
Line parameters for the low voltage distribution grid from [26].

| Bus from | Bus to | Resistance $R_{ph}$ (p.u.) | Reactance $X_{ph}$ (p.u.) |
|---|---|---|---|
| 1 | 2 | 0.012425 | 0.00363125 |
| 2 | 3 | 0.0062125 | 0.001815625 |
| 3 | 4 | 0.02174375 | 0.0037625 |
| 3 | 5 | 0.012425 | 0.00363125 |
| 5 | 6 | 0.0186375 | 0.005446875 |
| 6 | 7 | 0.0062125 | 0.001815625 |
| $S_{base}$ | 100 kV A | $V_{base}$ | 0.4 kV |

**Table 6**
NSGA-II parameter values used.

| Parameter | Value |
|---|---|
| Population size | 100 |
| Number of generations | 100 |
| Crossover probability | 0.9 |
| Mutation probability | 0.5 |
| Mutation distribution $\eta_m$ | 10 |

range of ±10% of the nominal voltage; voltage magnitudes are within ±2.5% with coefficient of determination of 0.975. Current magnitudes are within ±5% error limit with coefficient of determination of 0.964. There are values with error larger than 5% in the lower value range, but as mentioned before, it does not influence the accuracy of the whole model because only values near the maximum current magnitude are important. This can be improved by adding more segments at the lower values for approximating the quadratic function. However, this would increase the complexity of the model by adding significant number of additional variables. In conclusion, it was shown that the linearized AC power flow series of approximations for obtaining branch current magnitude are very accurate.

### 4.4. Combined method

The Pareto front of solutions (green dots) for the combined method is given in Fig. 12. There were 97 unique solutions. Gray dots show all evaluated solutions and red crosses are solutions that violated current constraints in the non-linear AC power flow calculation (voltage constraints were never violated). For the violated solutions, the optimal design and operation satisfy the linearized AC power flow constraints but are not feasible when the nonlinear AC power flow is calculated due to small errors from the linearization and approximation methods. Violated solutions are not present near the Pareto front but at higher cost regions that are far from optimal. The total cost for the lowest cost solution is 72 k€/a with carbon emissions of 218 tons/a. The carbon emissions can be decreased by 59% to 90 ton/a (the lowest carbon solution) by increasing the total cost by 27% to 91 k€/a.

### 4.5. Comparison of methods

Fig. 13 shows the Pareto fronts of all methods plotted in a single figure. Marked solutions (1 and 2) are example solutions that are analyzed in the next section. The MILP with linearized AC power flow method compared to the bi-level method gives similar cost range but the minimum achievable carbon emissions are smaller. This is because linear programming guarantees the global optimum whereas heuristics provide approximate solutions. Another reason is that in the bi-level method the optimal operation cannot be influenced in order to satisfy grid constraints. On the other

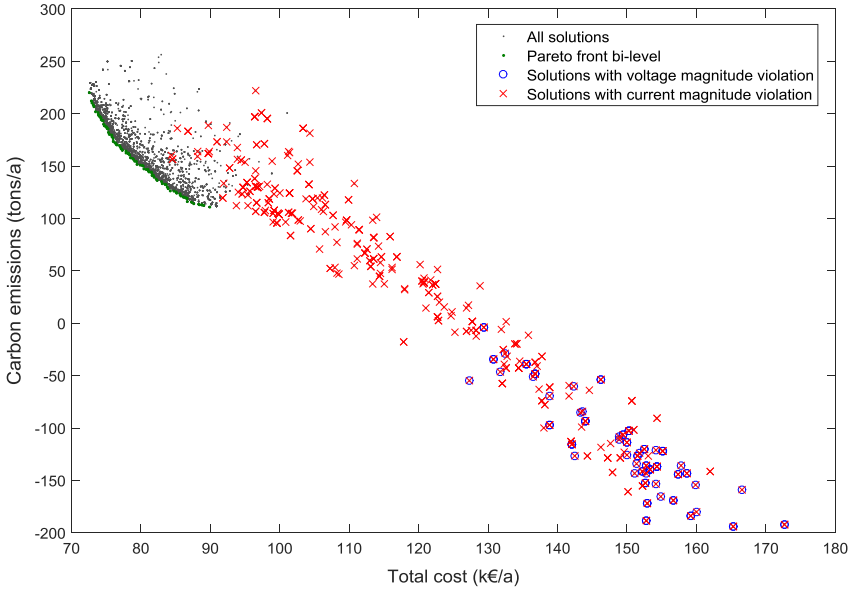


**Fig. 7.** Results of the bi-level optimization showing Pareto front, all solutions evaluated and solutions that violated each type of grid constraint.

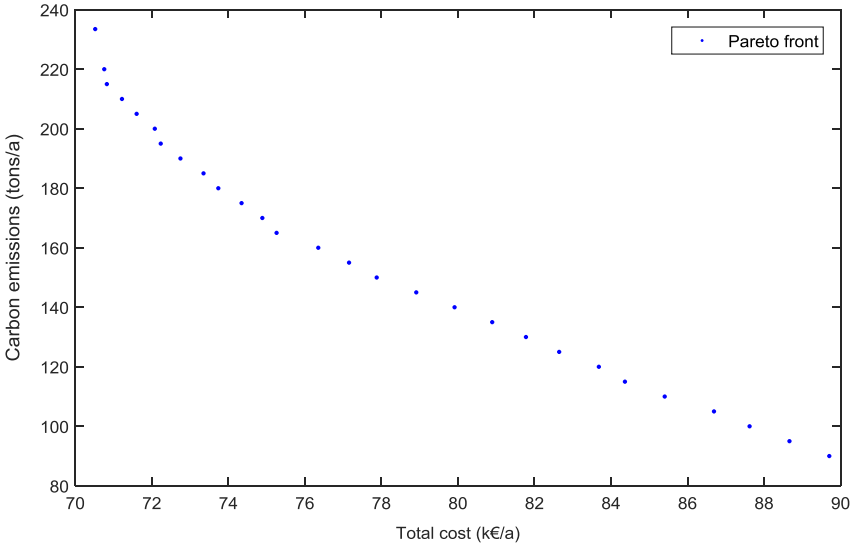


**Fig. 8.** Results of MILP with integrated linearized AC power flow optimization.

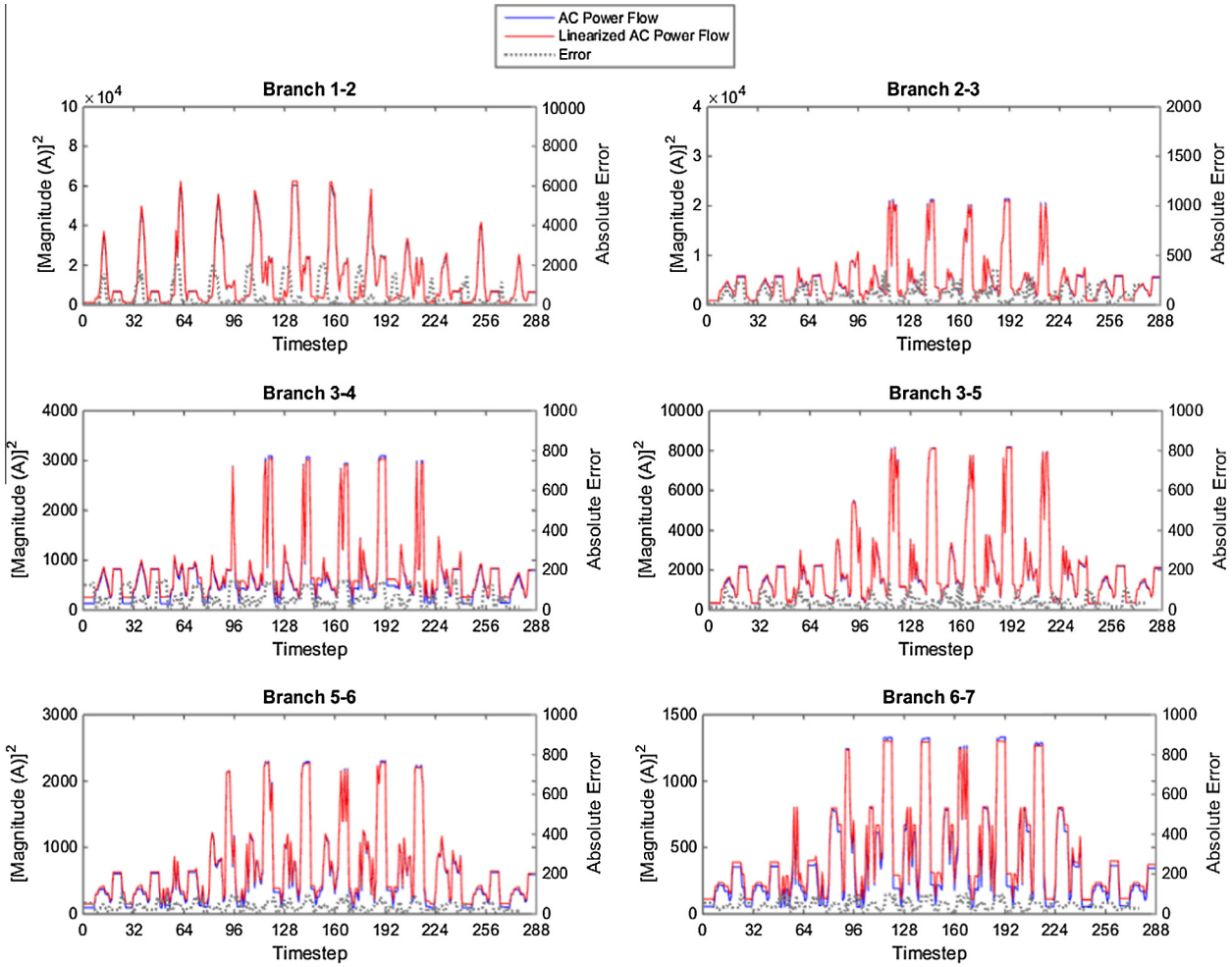


**Fig. 9.** Current magnitudes from non-linear AC power flow and linearized AC power flow calculations with absolute error.

hand, even though the MILP method gives the best results, there could be a possibility that certain results are violating the grid constraints due to errors in linearization. However, in this test case no solutions from the MILP method violated grid constraints when checked using the non-linear calculation.

Additionally, comparing the combined method to the MILP method with linearized AC power flows, the cost and emissions ranges are similar but the extreme solutions are slightly worse in both objectives. However, it gives better results than the bi-level method. Since the combined and bi-level methods are based on a

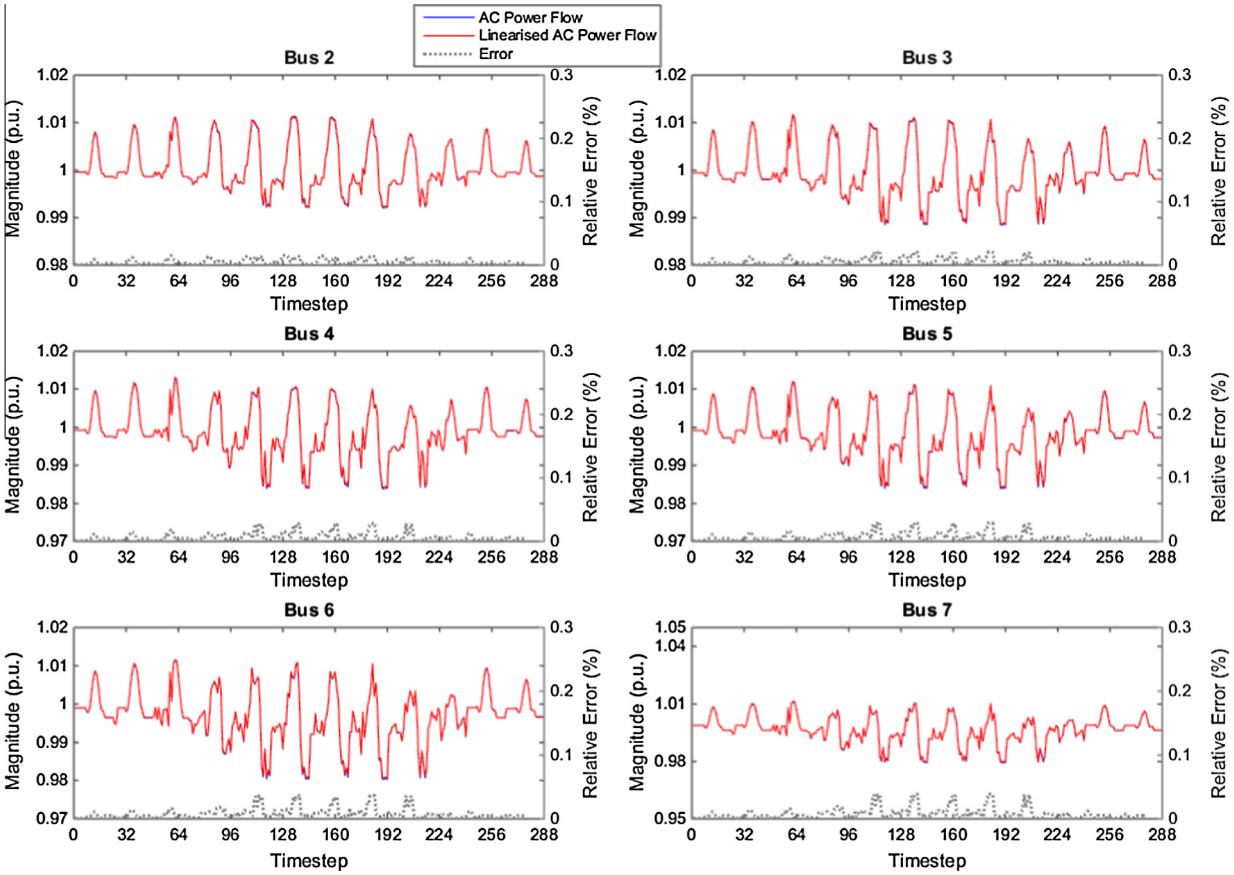


**Fig. 10.** Voltage magnitudes from non-linear AC power flow and linearized AC power flow calculations with relative error.

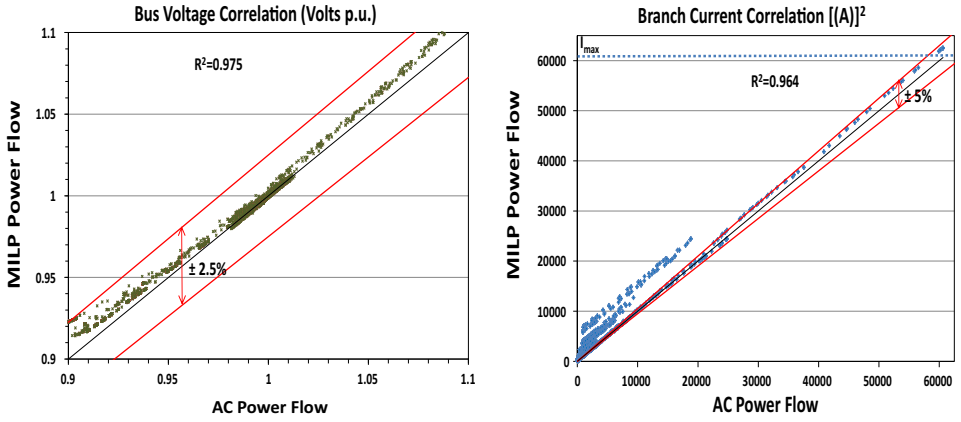


**Fig. 11.** Voltage and current correlation and error for non-linear AC power flow versus linearized power flow calculations. Red lines indicate region of error, the black line AC power flow result and $I_{max}$ the maximum current allowed by imposing constraint. (For interpretation of the references to color in this figure legend, the reader is referred to the web version of this article.)

heuristic algorithm, finding the global optimum cannot be guaranteed, but it can be seen that the Pareto fronts are relatively similar to that of the MILP method. Furthermore, the grid constraints are guaranteed not to be violated because of the nonlinear AC power flow calculation.

Finally, by integrating grid constraints in the operation optimization (MILP method) the minimum achievable carbon emissions decrease by 18% from 110 to 90 tons/a for the same cost compared to using an *a posteriori* check (bi-level method). For the combined method similar emissions are obtained but the cost is higher because it is based on approximate heuristics and not on exact linear programming.

Table 7 shows run times for each method. The optimization was performed on a PC with Intel i7 @2.70 GHz CPU and 16 GB RAM. The MILP with linearized AC power flows method had the shortest run time, and the combined method the longest. Run times of the

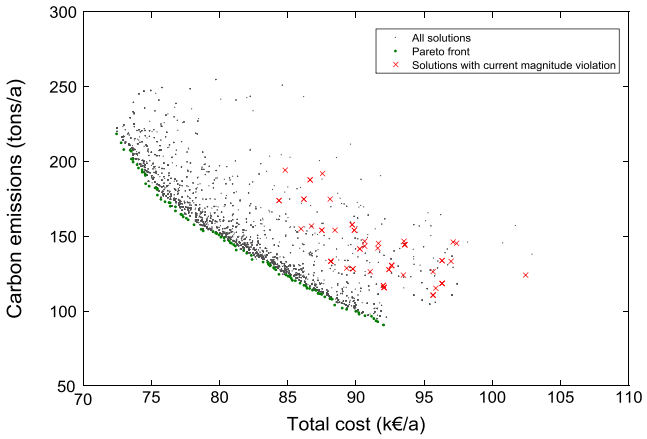


**Fig. 12.** Results of the combined method optimization showing Pareto front, all solutions evaluated and solutions that violated grid current constraints.

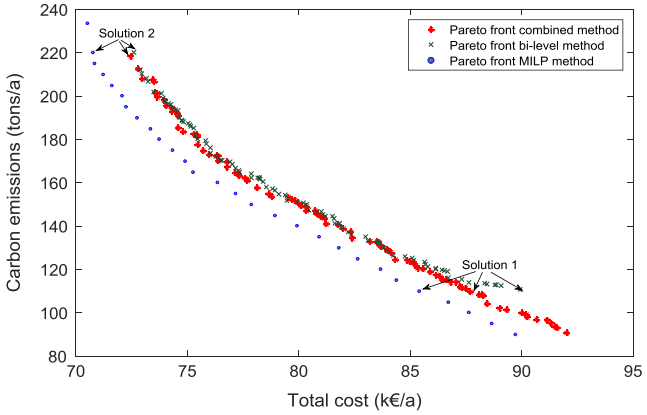


**Fig. 13.** Comparison of Pareto fronts of all methods. Example solutions that are analyzed in the next section are indicated.

**Table 7**
Run times of methods.

| Method | Run time (h) |
|---|---|
| Bi-level | 15 |
| MILP with linearized ACPF | 12 |
| Combined | 30 |

bi-level and combined methods are greatly influenced by the population size and number of generations, whereas for the MILP method the size of the problem is the important factor. However, in relative terms for small problems (1–7 buildings), the MILP method is the fastest.

### 4.6. Example solutions

Fig. 14 shows design variable, cost and emissions values for two solutions from each of the three methods (see Fig. 13), defined by carbon emissions value. The first solution is for carbon emissions of 110 tons/a and the second for 220 tons/a. In the first solution the bi-level method has the highest cost and the combined method the lowest cost. Gas boiler capacities are much higher in bi-level and combined methods. The reason is that the gas boiler is relatively cheap compared to other technologies and the influence on the cost is small so it is hard for the genetic algorithm to account for the difference. PV capacity is higher in the bi-level method and CHP capacity is lower compared to the other two methods, which have similar values. Looking at the second solution, the MILP method has the lowest cost. Similarly, the bi-level and combined methods have higher boiler capacities. The combined method has higher CHP and heat storage capacities.

Figs. 15 and 16 show a summary of operational variable values summed over a year for each method for both solutions. The operation of the MILP with linearized AC power flow and combined methods are similar, and different from the bi-level method in most of the variables. In solution 1, grid imports are the same but using the bi-level method less electricity is exported to the grid. Furthermore, gas boiler and PV are used less in the MILP and combined methods. Additionally, CHP and storage is used less in the bi-level method. Looking at solution 2, similar observations can be made but the differences are smaller.

In summary, PV is preferred over CHP, and the gas boiler is more used in the bi-level method. The reason is that CHP has more complex operation since it produces both electricity and heat, and also heat can be stored in heat storage. Without integrating grid constraints directly in the operation optimization (as with the MILP and combined methods), it is not possible to operate the CHP in such a way that it is complementary to PV production from the grid perspective and to decrease overall operating costs. That also is why the gas boiler is used more for satisfying heat demand in the bi-level method.

### 4.7. Discussion

An overview of the advantages and drawbacks of each method in terms of optimality, accuracy of the power flow and calculation time needed to solve small and large problems is given in Table 8. The methods are compared in a relative manner, not in absolute terms. Based on the results the following observations can be made:

- **Optimality:** The bi-level method has the worst performance. The global optimum cannot be guaranteed and operation is not influenced by the grid constraints. The MILP with linearized AC power flow method guarantees finding the global optimum and operation is influenced by the grid constraints. However,

| Solution | Method | Cost (k€/a) | Emissions (tons/a) | Gas boiler (kW) | PV (kWp) | CHP (kW) | Heat storage (kWh) |
|---|---|---|---|---|---|---|---|
| 1 | Bi-level | 89.92 | 110 | 949 | 173 | 71 | 254 |
| | MILP | 85.4 | 110 | 113 | 151 | 100 | 247 |
| | Combined | 87.71 | 110 | 703 | 155 | 99 | 281 |
| 2 | Bi-level | 72.59 | 220 | 749 | 4 | 66 | 218 |
| | MILP | 70.75 | 220 | 182 | 0 | 67 | 210 |
| | Combined | 72.45 | 220 | 623 | 0 | 76 | 270 |

**Fig. 14.** Design and objective values of the three methods for two solutions.

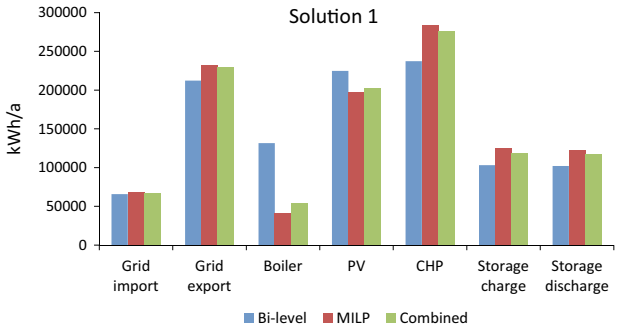


**Fig. 15.** Summary of operation variable values for solution 1 using each method.

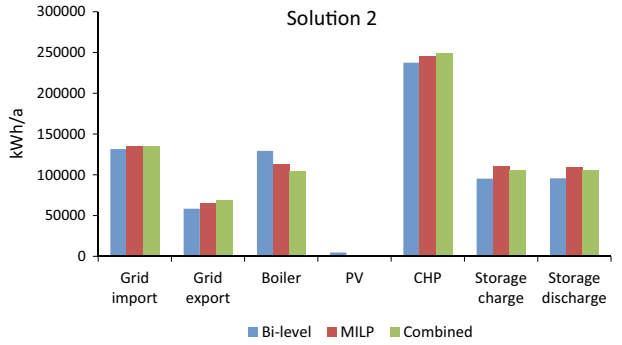


**Fig. 16.** Summary of operation variable values for solution 2 using each method.

there are small errors due to linearization approximations and there is a small possibility that not all solutions are feasible. As for the combined method, the global optimum cannot be guaranteed but operation is influenced by the grid constraints which provides solutions almost as good as the MILP method.

- **Accuracy of the power flow:** The bi-level method uses a nonlinear AC power flow calculation solved by the Newton-Raphson method, so grid constraints are fulfilled with certainty. The MILP with linearized AC power flow uses linearized AC power flow via series of approximations in order to obtain branch current. This introduces an error but from the results it can be seen that it is very small. The combined method uses both linearized AC power flow and nonlinear AC power flow calculations. This improves the optimality while guaranteeing the accuracy of the grid constraints.
- **Solving performance:** The bi-level method is efficient at solving both small and large problems. For large problems the solving time can increase a lot, however it does not have onerous hardware requirements. This means that each problem is solvable within a corresponding timeframe. The MILP with linearized AC power flow method uses a branch and cut algorithm to subdivide the problem. The algorithm efficiently solves small (1–15 buildings) to medium size problems (16–30 buildings). Large problems (31 + buildings) can be realistically unsolvable due to solving time but also due to hardware requirements; the larger the problem, the larger the branching tree required, and thus the larger the RAM requirement. Eventually the hardware requirements become unrealistic (e.g. 1 Tb of RAM). As for the combined method, it efficiently solves small problems but it has longer solving times for larger problems compared to the bi-level method due to the model being more complicated. On the other hand, it is not constrained by RAM requirements since it uses a heuristic as the solving algorithm. The solving time can be decreased by using a smaller population size and fewer generations, though this sacrifices some degree of optimality.

In conclusion, the bi-level method can be used for both small and large problems when a relatively quick and 'good enough' solution is needed with guaranteed accuracy of the power flow calculation. The MILP with linearized AC power flow method can be used for efficiently solving small problem when a guaranteed global optimum is needed and 'good enough' accuracy of the power flow is sufficient. For large problems, realistic solvability is case specific. The combined method provides best general performance overall. It provides near globally optimal solutions with guaranteed accuracy of the power flow calculation. Also, it efficiently solves both small and large problems. The drawback is that the solving time is higher than the bi-level method, but on the other hand is not limited by hardware like the MILP method.

The comparison showed that in order to increase the share of renewable energy sources and other local generations, distribution grid upgrades are often important. Integrating grid constraints in the operational optimization gives much better results compared to checking them *a posteriori*. In this specific case, the carbon emissions objective improved from 110 to 90 tons/a (a difference of 18%). All this highlights why it is important to include grid constraints in the optimization of distributed energy systems.

## 5. Mitigating the impact of distributed energy systems on the distribution grid

This section investigates the problems that arise from large scale integration of DES in the distribution grid as well as how much can the negative impact of distributed generation on the distribution grid can be mitigated and grid upgrades avoided by taking into account grid constraints when designing and determining

**Table 8**
Relative comparison of the methods in terms of optimality, accuracy of the power flow calculation and solving time.

| Methods | Optimality | Accuracy of the power flow | Solving performance | |
|---|---|---|---|---|
| | | | Small Problems | Large Problems |
| Bi-level | - | + | + | + |
| MILP with linearized AC power flow | + | +/- | + | - |
| Combined | +* | + | +/- | +/- |

Legend: – worst performance, ±average performance, +* near best performance, + best performance.

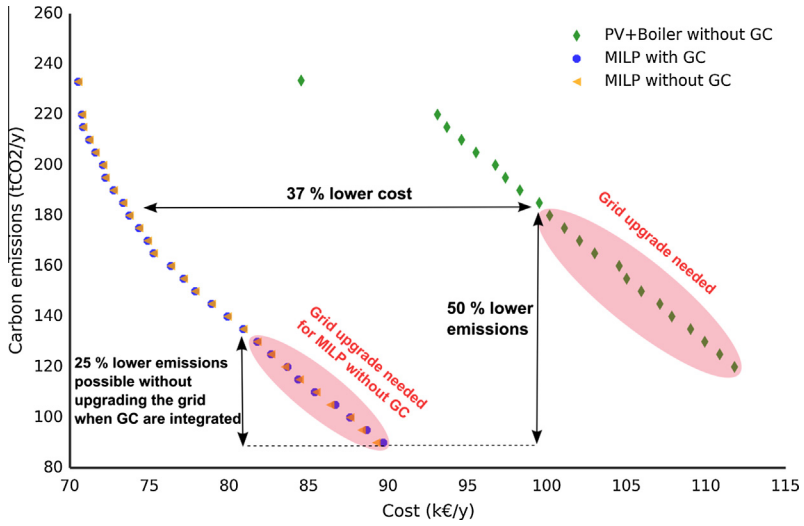


**Fig. 17.** Comparison of Pareto fronts of all scenarios. Red crosses mark the solutions that require grid upgrade in order to be feasible. (For interpretation of the references to color in this figure legend, the reader is referred to the web version of this article.)

**Table 9**
Maximum possible PV capacity that can be integrated and maximum decrease in carbon emissions without upgrading the grid.

| | PV + Boiler without GC | MILP without GC | MILP with GC |
|---|---|---|---|
| Integrated PV capacity (kWp) | 174 | 220 | 300 |
| Decrease in carbon emissions (%) | 20 | 40 | 60 |

operation strategies of DES. Three scenarios have been run using the case study presented in Section 3:

1. **PV + Boiler without GC:** The most common approach to decreasing the carbon emissions is to install PV in addition to existing building systems. In this scenario it is assumed that a gas boiler is used for meeting heat demand and electricity from the grid or from PV meets the electric demand. Electrical grid constraints are not considered. This scenario acts as a base case representing typical current practice.
2. **MILP without GC:** In this scenario all technologies are optimized (gas boiler, PV, CHP, heat storage) for meeting demands. But, grid constraints are not considered. This case represents a state-of-the-art optimization study.
3. **MILP with GC:** In this scenario all technologies are considered as well as grid constraints are integrated using the MILP method from the previous section. This case highlights the importance of including grid constraints.

Fig. 17 shows the Pareto fronts of all scenarios. The MILP with GC and without GC scenarios are up to 37% less expensive for the same carbon limits and can achieve lower carbon emissions compared to the PV + Boiler without GC scenario. This is because using the technologies that produce both electricity and heat combined with heat storage, provides more flexibility in meeting the energy demands and thus more heat and electricity can be locally produced. When grid constraints are not considered, the results show that carbon emissions can be decreased to 120 $tCO_2/y$ in PV + Boiler without GC scenario and to 90 $tCO_2/y$ in MILP without GC. But solutions with lower emissions require grid upgrade. It is only possible to decrease carbon emissions to 180 $tCO_2/y$ for PV + Boiler without GC and 121 $tCO_2/y$ for the MILP without GC scenario if grid is not upgraded. On the other hand, the MILP with GC scenario can achieve 90 $tCO_2/y$ without grid upgrade with similar cost. Table 9 shows how much PV can be integrated and the relative carbon emissions reductions possible without upgrading the grid for each scenario. The capacity of integrated PV can be increased 20% from 174 kWp to 220 kWp when all technologies are considered and additionally 25% to 300 kWp when grid constraints are also taken into account. Carbon emissions can be reduced 20–40% and additionally to 60% consequently.

The total cost of upgrading the analyzed grid is 52 k€ which consists of installing 0.4 kV 240Al lines with a price of 80 k€/km and upgrading the transformer to 630 kV A with a price of 21 k€ [40]. These costs should be included when evaluating other scenarios, which can change the favorable strategy. However, the total cost should not be the only criteria when deciding how to decrease carbon emissions. Voltage levels and branch currents should also be considered.

The frequency of different voltage levels for a carbon limit of 120 $tCO_2/y$ for the MILP with GC and PV + Boiler without GC scenarios are shown in Fig. 18. Bus numbers correspond to those in Fig. 6. It can be seen that the voltage variations are the biggest in the end buses because of voltage drops in the cable. More often there is a case of over-voltage than under-voltage which is associated with increased PV integration. Under- or over-voltages can cause problems such as equipment malfunction, overloading of induction motors and higher losses in transformers [41]. It can be seen that in the MILP with GC scenarios, voltages are more closely grouped around 1 p.u. in all buses. For the same amount of PV integration, considering grid constraints leads to much less negative impact on the voltage levels and as consequence improves the reliability of the grid and equipment.

Total current values at each branch have been depicted in Fig. 19 for all three scenarios for a carbon limit of 120 $tCO_2/y$. Each branch is denoted by two numbers which correspond to bus numbers in Fig. 6. The maximum allowed current of 250 A is also marked. As expected the currents are the highest in the first branch. In the MILP with GC scenario the maximum current value is never exceeded. However, in the PV + Boiler without GC scenario there are many outliers that exceed the maximum current. The reason is that in this scenario the only way to decrease carbon emissions is to integrate a large amount of PV. As a consequence during the summer periods there is a lot of generation from PV that exceeds the maximum allowed current. Also, the median, lower

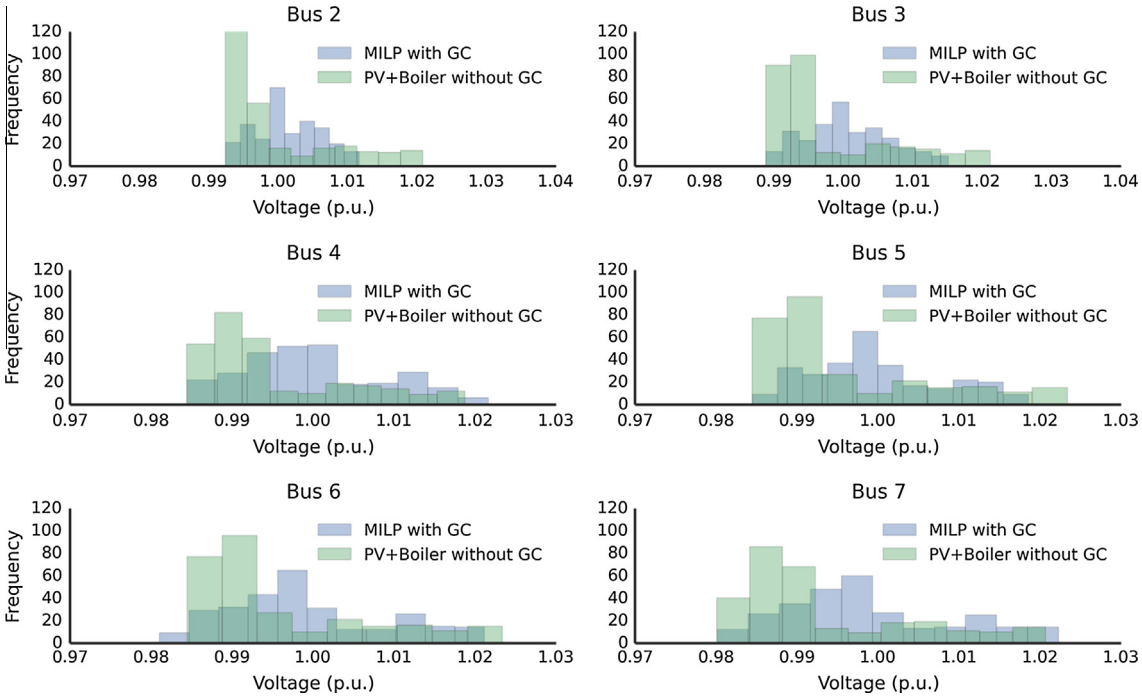


**Fig. 18.** Histogram of voltage deviations of all buses for carbon emissions limit of 120 $tCO_2$/y.

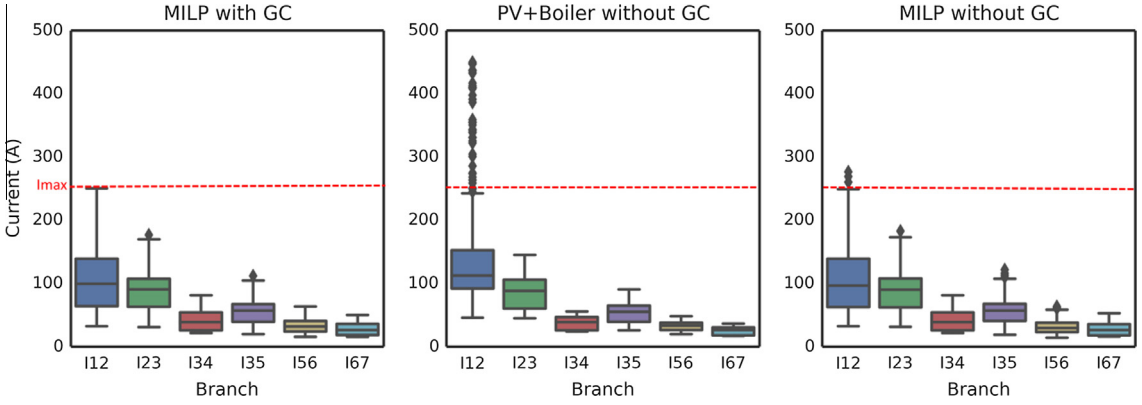


**Fig. 19.** Total currents in each branch for carbon emissions limit of 120 $tCO_2$/y.

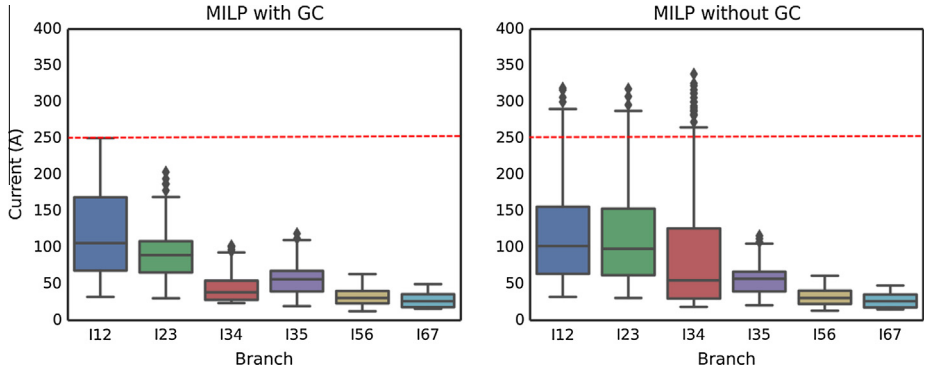


**Fig. 20.** Total currents in each branch for carbon emissions limit of 90 $tCO_2$/y.

quartile and upper quartile are higher which indicates overall higher currents. Looking at the MILP without GC case it is similar to the MILP with GC case, but with some outliers exceeding the current limit in the first branch. This is because other technologies are available and hence integrating a large share of PV is not the only way to reduce carbon emissions.

However, when carbon emissions are further decreased the impact of DES on the grid becomes evident if not managed properly. Fig. 20 shows total currents for a carbon limit of 90 $tCO_2$/y for the MILP scenarios with and without GC. It can be seen that without GC the currents in the grid are significantly larger. In the first three branches, the maximum exceeds the stable current limit with outliers being even higher. The medians and interquartile ranges are also higher than the scenarios with GC. Increased currents can decrease the flexibility of the grid and increase short circuit currents. Also, currents above rated levels result in overheating and shortened life expectancies of the transformer and cables which increase the grid operating costs [42]. Furthermore, it decreases the potential for future integration of additional local generation and electric vehicles.

In summary, the results show that the impact of DES on the distribution grid can be significant and may have negative consequence on the cables, transformer and equipment if not managed properly. This can increase the overall cost and decrease the flexibility and reliability of the distribution grid. The negative impact is more connected with current problems than with voltage problems. This is in line with the general rule that the voltage problems are characteristic of high length networks (total length more than 400 m). On the other hand, the current problems and transformer reinforcements are generally characteristic for short networks (total length less than 300 m) [40]. The length of the analyzed grid is 200 m. Finally, the results highlighted that by integrating grid constraints and properly managing power flows, it is possible to significantly decrease voltage and current problems, and avoid grid upgrades while simultaneously integrating large share of PV. This can help achieve cost effective reduction of carbon emissions.

## 7. Conclusions

An integrated optimization framework that incorporates the optimal design and operation of DES combined with electrical grid constraints, building simulation and interactions between various energy streams is described. It consists of building energy simulations for obtaining demand profiles, energy hub models for design and operation of building systems and a distribution grid model for power flow studies of grid stability constraints.

Three methods in which grid constraints can be integrated in the optimization model are outlined. The first method is based on bi-level optimization where the grid model and constraints are separate from the energy hub model. The second method is based on the integration of the linearized AC power flow equations and constraints directly within the energy hub model. The third method combines the approaches of the previous two methods. The optimality, accuracy of the power flow calculations and solving performance of the methods were examined on a test case. The bi-level method quickly provides 'good enough' solutions with accurate power flow calculation. The MILP with linearized AC power flow method gives globally optimal solutions with possible small errors in the power flow constraints. Moreover, it efficiently solves small problems but is limited by hardware for large problems. The combined method gives near optimal solutions with accurate power flow. It is not limited by hardware for large problems, but the solving time is higher than the bi-level method. The comparison indicated that the suitability of a specific method is dependent on the application. Therefore, it is up to the user to choose the best method based on the individual criteria.

The results of the test case showed that there are a large number of solutions that are optimal in terms of the distributed energy system but are not feasible from the distribution grid perspective. This shows the importance of including the electricity grid constraints in the design of distributed energy systems. Integrating grid constraints directly into the operational optimization achieved additional savings of 18% in carbon emissions for the same cost compared to *a posteriori* checking. Furthermore, it was shown that by properly designing and determining operation schedule of DES, it is possible to decrease voltage variations and currents in the grid. The negative impacts on the grid are mostly connected with exceeding current limits, which is expected for short grids. Also, 45% more renewables can be integrated and carbon emissions decreased 40% without grid upgrades when DES is considered and grid constraints in the operation scheduling are implemented.

In the future work the possibility of upgrading grid sections (with associated costs) will be included, as well as consideration of heat and gas networks. Also, the options of battery storage and demand response measures will be added along with time-of-use electricity pricing strategies.

## Acknowledgment

This research has been financially supported by CTI within the SCCER FEEB&D (CTI.2014.0119).

## References

[1] Manfren M, Caputo P, Costa G. Paradigm shift in urban energy systems through distributed generation: methods and models. Appl Energy 2011;88(4):1032–48.
[2] Stadler M, Groissböck M, Cardoso G, Marnay C. Optimizing distributed energy resources and building retrofits with the strategic DER-CAModel. Appl Energy 2014;132:557–67.
[3] Ren H, Gao W. A MILP model for integrated plan and evaluation of distributed energy systems. Appl Energy 2010;87(3):1001–14.
[4] Ren H, Zhou W, Nakagami K, Gao W, Wu Q. Multi-objective optimization for the operation of distributed energy systems considering economic and environmental aspects. Appl Energy 2010;87(12):3642–51.
[5] Mehleri ED, Sarimveis H, Markatos NC, Papageorgiou LG. A mathematical programming approach for optimal design of distributed energy systems at the neighbourhood level. Energy 2012;44(1):96–104.
[6] Omu A, Choudhary R, Boies A. Distributed energy resource system optimisation using mixed integer linear programming. Energy Policy 2013;61:249–66.
[7] Holjevac N, Capuder T, Kuzle I. Adaptive control for evaluation of flexibility benefits in microgrid systems. Energy 2015.
[8] Chen Y-H, Lu S-Y, Chang Y-R, Lee T-T, Hu M-C. Economic analysis and optimal energy management models for microgrid systems: a case study in Taiwan. Appl Energy 2013;103:145–54.
[9] Calvillo CF, Sánchez-Miralles A, Villar J. Assessing low voltage network constraints in distributed energy resources planning. Energy 2015;84:783–93.
[10] Thomson M, Infield D. Modelling the impact of micro-combined heat and power generators on electricity distribution networks. Proc Inst Mech Eng Part A J Power Energy 2008;222(7):697–706.
[11] Cossent R, Olmos L, Gómez T, Mateo C, Frías P. Distribution network costs under different penetration levels of distributed generation. Eur Trans Electr Power 2011;21(6):1869–88.
[12] Liu X, Wu J, Jenkins N, Bagdanavicius A. Combined analysis of electricity and heat networks. Appl Energy 2016;162:1238–50.
[13] Mancarella P, Gan CK, Member S, Strbac G. Evaluation of the impact of electric heat pumps and distributed CHP on LV networks. In: PowerTech conference in Trondheim; 2011. p. 1–7.
[14] Baetens R, De Coninck R, Van Roy J, Verbruggen B, Driesen J, Helsen L, et al. Assessing electrical bottlenecks at feeder level for residential net zero-energy buildings by integrated system simulation. Appl Energy 2012;96:74–83.
[15] Thomson M, Infield DG. Impact of widespread photovoltaics generation on distribution systems. IET Renew Power Gener 2007;1(1):33.
[16] Navarro-Espinosa A, Mancarella P. Probabilistic modeling and assessment of the impact of electric heat pumps on low voltage distribution networks. Appl Energy 2014;127:249–66.
[17] Pękala ŁM, Tan RR, Foo DCY, Jeżowski JM. Optimal energy planning models with carbon footprint constraints. Appl Energy 2010;87(6):1903–10.
[18] Rees MT, Wu J, Jenkins N, Abeysekera M. Carbon constrained design of energy infrastructure for new build schemes. Appl Energy 2014;113:1220–34.
[19] Blarke MB. Towards an intermittency-friendly energy system: comparing electric boilers and heat pumps in distributed cogeneration. Appl Energy 2012;91(1):349–65.
[20] Yang Y, Zhang S, Xiao Y. Optimal design of distributed energy resource systems coupled with energy distribution networks. Energy 2015;85:433–48.
[21] Kopanos GM, Georgiadis MC, Pistikopoulos EN. Energy production planning of a network of micro combined heat and power generators. Appl Energy 2012;102(2013):1522–34.

[22] Viral R, Khatod DK. Optimal planning of distributed generation systems in distribution system: a review. Renew Sustain Energy Rev 2012;16 (7):5146–65. Sep.
[23] Abdullah MA, Agalgaonkar AP, Muttaqi KM. Assessment of energy supply and continuity of service in distribution network with renewable distributed generation. Appl Energy 2014;113:1015–26.
[24] Purchala K, Meeus L, Van Dommelen D, Belmans R. Usefulness of DC power flow for active power flow analysis. In: Power engineering society general meeting, 2005, vol. 1. IEEE; 2005. p. 454–9.
[25] Stott B, Jardim J, Alsac O. DC Power Flow Revisited. IEEE Trans Power Syst 2009;24(3):1290–300.
[26] Koster AMCA, Lemkens S. In: Pahl J, Reiners T, Voß S, editors. Network optimization: 5th international conference, INOC 2011, Hamburg, Germany, June 13–16, 2011. Proceedings. Berlin, Heidelberg: Springer Berlin Heidelberg; 2011. p. 478–83.
[27] Geidl M, Andersson G. Optimal coupling of energy infrastructures. In: 2007 IEEE lausanne power tech; 2007. p. 1398–403.
[28] Haimes YY, Lasdon LS, Wismer DA. On a bicriterion formulation of the problems of integrated system identification and system optimization. Syst, Man Cybernetics, IEEE Trans, vol. SMC-1, no. 3; 1971. p. 296–7.
[29] Morvaj B, Evins R, Carmeliet J. Optimisation framework for distributed energy systems with integrated electrical grid constraints. Energy 2016. submited to.
[30] Evins R, Orehounig K, Dorer V, Carmeliet J. New formulations of the 'energy hub' model to address operational constraints. Energy 2014;73:387–98.
[31] Deb K, Pratap A, Agarwal S, Meyarivan T. A fast and elitist multiobjective genetic algorithm: NSGA-II. IEEE Trans Evol Comput 2002;6(2):182–97.
[32] Zimmerman RD, Murillo-Sánchez CE, Thomas RJ. MATPOWER: steady-state operations, planning, and analysis tools for power systems research and education. Power Syst IEEE Trans 2011;26(1):12–9.
[33] Williams HP. Model building in mathematical programming. 5th ed. Wiley; 2013.
[34] Crawley DB, Lawrie LK, Winkelmann FC, Buhl WF, Huang YJ, Pedersen CO, et al. EnergyPlus: creating a new-generation building energy simulation program. Energy Build 2001;33(4):319–31.
[35] Technical annex to the SEAP template instructions document: THE EMISSION FACTORS.
[36] Brander M, Sood A, Wylie C, Haughton A, Lovell J. Electricity specific emission factors for grid electricity; 2011. <http://ecometrica.com/assets/Electricity-specific-emission-factors-for-grid-electricity.pdf>.
[37] Energy price statistics. <http://epp.eurostat.ec.europa.eu/statistics_explained/index.php/energy_price_statistics#Electricity_prices_for_household_consumers>. [accessed: 12-Nov-2014].
[38] Papathanassiou S, Hatziargyriou N, Strunz K. A benchmark low voltage microgrid network. In: Proceedings of the CIGRE symposium: power systems with dispersed generation; 2005. p. 1–8.
[39] Marszal J, Heiselberg P, Bourrelle JS, Musall E, Voss K, Sartori I, et al. Zero energy building – a review of definitions and calculation methodologies. Energy Build 2011;43(4):971–9.
[40] Mehmedalic J, Rasmussen J, Harbo S, Association DE. Reinforcement costs in low-voltage grids; 2013. <http://www.greenemotion-project.eu/upload/pdf/deliverables/D4_3_B2-Grid-Impact-studies-of-electric-vehicles-Reinforcement-costs-in-LV-Grids-V1_1_submitted.pdf>.
[41] Short T. Voltage regulation. CRC Press; 2014.
[42] Knezovic K, Marinelli M, Codani P, Perez Y. Distribution grid services and flexibility provision by electric vehicles: A review of options. In: Power engineering conference (UPEC), 2015 50th international universities; 2015. p. 1–6.
[43] Mehleri ED, Sarimveis H, Markatos NC, Papageorgiou LG. Optimal design and operation of distributed energy systems: application to Greek residential sector. Renew Energy 2013;51:331–42.
[44] Lund H, Möller B, Mathiesen BV, Dyrelund a. The role of district heating in future renewable energy systems. Energy 2010;35(3):1381–90.